

Analysis and Optimization of a DAR IMPATT Diode for 330 GHz

ALEXANDER ZEMLIAK^{1,3}, ANDREY OSTROVSKY¹, SERGIO VERGARA²,
EVGENIY MACHUSSKIY³

¹Department of Physics and Mathematics

²Department of Electronics

Autonomous University of Puebla

Av. San Claudio y Rio Verde, Puebla, 72570

MEXICO

³Institute of Physics and Technology

National Technical University of Ukraine

UKRAINE

azemliak@cfm.buap.mx, andreyo@cfm.buap.mx, svergara@ece.buap.mx,
shtorm@uap.ntu-kpi.kiev.ua

Abstract: - The analysis and optimization of the n^+pvnp^+ avalanche diode have been realized on basis of the nonlinear model and special optimization procedure. This type of the diode that was named as Double Avalanche Region (DAR) IMPATT diode includes two avalanche regions inside the diode. The phase delay which was produced by means of the two avalanche regions and the drift region v is sufficient to obtain the negative resistance for the wide frequency band. The admittance and energy characteristics of the DAR diode were analyzed in very wide frequency band from 30 up to 360 GHz. Output power level was optimized for the third frequency band near the 330 GHz.

Key Words: - Implicit numerical scheme, active layer structure optimization, DAR IMPATT diode.

1 Introduction

One of the important problems of modern microwave electronics concerns of the power generation of sufficient output level of millimeter region. The IMPATT diodes of different structures are used very frequently in microwave systems. The single drift region (SDR) and the double drift region (DDR) IMPATT diodes are very well known and used successfully for the microwave power generation in millimeter region [1-3]. From the famous paper of Read [4] the main idea to obtain the negative resistance was defined on the basis of the phase difference being produced between RF voltage and RF current due to delay in the avalanche build-up process and the transit time of charge carriers. The transit time delay of both types of diodes (SDR and DDR) is the essential factor of the necessary phase conditions to obtain negative resistance. However an IMPATT diode that has double avalanche regions (DAR) can produce an avalanche delay which alone can satisfy conditions necessary to generate microwave power [5-9]. The DAR diode can be defined for instance by means of the structure n^+pvnp^+ in Fig. 1. This diode has two avalanche regions around n^+p and np^+ junctions and one common drift region. This type of diode was suggested in [5]. The characteristics of this diode

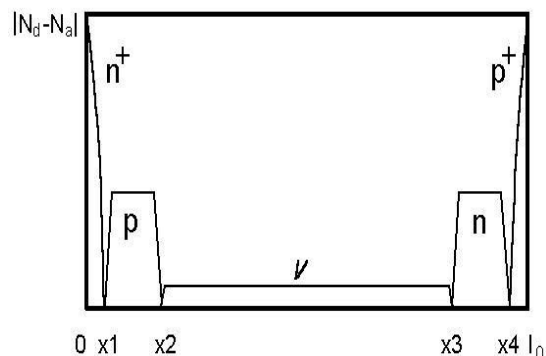


Figure 1. Doping profile for DAR IMPATT diode.

were analyzed in DC and RF modes [6-9]. The authors affirm that the avalanche delay produced by each of the thin avalanche regions becomes nearly $\pi/2$, making the total avalanche delay equal to π that is sufficient to produce negative diode resistance.

The frequency characteristics of this diode were analyzed in [9] by means of approximate model. The authors said that the diode active properties are produced in many frequency bands for any drift zone width. Our preliminary analysis obtained on basis of the sufficiently precise model [10, 11] contradicts to the results [9].

2 Nonlinear Model

The drift-diffusion model which is used for the diode analysis consists of two continuity equations for the electrons and holes, the Poisson equation for the potential distribution in semiconductor structure and necessary boundary conditions as for continuity equations and for the Poisson equation. The principal equations can be presented in next form:

$$\begin{aligned} \frac{\partial n(x,t)}{\partial t} &= \frac{\partial J_n(x,t)}{\partial x} + \alpha_n |J_n(x,t)| + \alpha_p |J_p(x,t)| \\ \frac{\partial p(x,t)}{\partial t} &= -\frac{\partial J_p(x,t)}{\partial x} + \alpha_n |J_n(x,t)| + \alpha_p |J_p(x,t)| \\ J_n(x,t) &= n(x,t) V_n + D_n \frac{\partial n(x,t)}{\partial x} \\ J_p(x,t) &= p(x,t) V_p - D_p \frac{\partial p(x,t)}{\partial x} \end{aligned} \quad (1)$$

where n, p are the concentrations of electrons and holes; J_n, J_p are the current densities; α_n, α_p are the ionization coefficients; V_n, V_p are the drift velocities; D_n, D_p are the diffusion coefficients. The dependences of the ionization coefficients on field and temperature and charge transport properties have been approximated using the approach in [12-15].

The boundary conditions for this system include concentration and current definition for contact points and can be written as follows:

$$\begin{aligned} n(0,t) &= N_D(0); & p(l_0,t) &= N_A(l_0); \\ J_n(l_0,t) &= J_{ns}; & J_p(0,t) &= J_{ps}. \end{aligned} \quad (2)$$

where J_{ns}, J_{ps} are the electron current and the hole current for inversely biased $p-n$ junction; $N_D(0), N_A(l_0)$ are the concentrations of donors and acceptors at two end space points $x=0$ and $x=l_0$; where l_0 is the length of the active layer of semiconductor structure.

The electrical field distribution in semiconductor structure can be obtained from the Poisson equation. As electron and hole concentrations are functions of the time, therefore, this equation is the time dependent too and time is the equation parameter. The Poisson equation for the above defined problem has the following normalized form:

$$\frac{\partial E(x,t)}{\partial x} = -\frac{\partial^2 U(x,t)}{\partial x^2} = N_D(x) - N_A(x) + p(x,t) - n(x,t) \quad (3)$$

where $N_D(x), N_A(x)$ are the concentrations of donors and acceptors accordingly, $U(x,t)$ is the potential, $E(x,t)$ is the electrical field. The boundary conditions for this equation are:

$$U(0,t) = 0; \quad U(l_0,t) = U_0 + \sum_{m=1}^M U_m \sin(\omega mt + \varphi_m) \quad (4)$$

where U_0 is the DC voltage on diode contacts; U_m is the amplitude of harmonic number m in diode contacts; ω is the fundamental frequency; φ_m is the phase of harmonic number m ; M is the number of harmonics. In this paper we analyze one harmonic regime only ($M=1$) and in this case the phase φ_m can be define as 0. Concrete values of the voltages U_0, U_1 and frequency ω have been defined during the analysis in section 5. Equations (1)-(4) adequately describe processes in the IMPATT diode in a wide frequency band. However, numerical solution of this system of equations is very difficult due to existing of a sharp dependence of equation coefficients on electric field. Explicit numerical schemes have poor stability and require a lot of computing time for good calculation accuracy obtaining [16]. It is more advantageous to use implicit numerical scheme that has a significant property of absolute stability. Computational efficiency and numerical algorithm accuracy are improved by applying the space and the time coordinates symmetric approximation.

After approximation of functions and its differentials the system (1) is transformed to the implicit modified Crank-Nicholson numerical scheme. This modification consists of two numerical systems each of them having three-diagonal matrix. These systems have the following form:

$$\begin{aligned} -(a_n - b_n) n_{i-1}^{k+1} + (1+2a_n) n_i^{k+1} - (a_n + b_n) n_{i+1}^{k+1} = \\ a_n n_{i-1}^k + (1-2a_n) n_i^k + a_n n_{i+1}^k + b_n (n_{i+1}^k - n_{i-1}^k) \\ + \alpha_n \left[\tau \cdot V_n \cdot n_i^k + r \cdot D_n \cdot (n_{i+1}^k - n_{i-1}^k) \right] \\ + \alpha_p \left[\tau \cdot V_p \cdot p_i^k - r \cdot D_p \cdot (p_{i+1}^k - p_{i-1}^k) \right] \\ -(a_p + b_p) p_{i-1}^{k+1} + (1+2a_p) p_i^{k+1} - (a_p - b_p) p_{i+1}^{k+1} = \\ a_p p_{i-1}^k + (1-2a_p) p_i^k + a_p p_{i+1}^k - b_p (p_{i+1}^k - p_{i-1}^k) \\ + \alpha_p \left[\tau \cdot V_p \cdot p_i^k - r \cdot D_p \cdot (p_{i+1}^k - p_{i-1}^k) \right] \\ + \alpha_n \left[\tau \cdot V_n \cdot n_i^k + r \cdot D_n \cdot (n_{i+1}^k - n_{i-1}^k) \right] \\ i = 1, 2, \dots, I_1 - 1; \quad k = 0, 1, 2, \dots, \infty \end{aligned} \quad (5)$$

where $a_{n,p} = \frac{\tau D_{n,p}}{2h^2}$; $b_{n,p} = \frac{\tau V_{n,p}}{4h}$; $r = \frac{\tau}{2h}$; i is the space coordinate current node number; k is the time coordinate node number; h is the space step; τ is the time step; I_1 is the space node number.

The approximation of the Poisson equation is performed using ordinary finite difference scheme at every time step k :

$$U_{i-1}^k - 2U_i^k + U_{i+1}^k = h^2(N_{Di} - N_{Ai} + p_i^k - n_i^k) \quad (6)$$

Numerical algorithm for the calculation of IMPATT diode characteristics consists of the following stages: 1) the voltage is calculated at the diode contacts for every time step by formula (4); 2) the voltage distribution is calculated at every space point from the Poisson equation (6) by factorization method [17], the electrical field distribution along the diode active layer is calculated; 3) the charge carries ionization and drift parameters are calculated in numerical net nodes for the current time step; 4) the system of equations (5) is solved by matrix factorization method taking into account the boundary conditions (2) and electron and hole concentration distributions are calculated for the new time step and than the calculation cycle is repeated for all time steps until the end of the time period; 5) the full current in external circuit is calculated taking into account a series resistance R_s ($R_s = 0.5_{10-6}$ Ohm \cdot cm²), which reflects losses in semiconductor structure. This process is continued from one period to another until the convergence is achieved by means of the results comparison for the two neighboring periods with the necessary precision. Then all harmonics of the external current, admittance for the harmonic number m and power characteristics can be calculated by the Fourier transformation.

3 Optimization Technique

The special optimization algorithm that combines one kind of direct method and a gradient method was used to optimize the output characteristics of DAR diode. To obtain the better solution for the optimum procedure, it is necessary to analyze N -dimensional space for $N=5$. The principal vector of optimization parameters consists of five variables $y = (y_1, y_2, y_3, y_4, y_5)$, where the components will be defined below. The optimization algorithm can be defined by next steps:

1. Given as input two different approximations of two initial points Y^0 and Y^1 .

2. At these points, we start with the gradient method, and have performed some steps. As a result, we have two new points Y^0 and Y^1 . This process is reflected by the next equations:

$$\begin{aligned} y^{0,n+1} &= y^{0,n} - \delta_n \cdot \nabla F(y^{0,n}), \\ y^{1,n+1} &= y^{1,n} - \delta_n \cdot \nabla F(y^{1,n}), \end{aligned} \quad (7)$$

$$n=0, 1, \dots, N-1$$

$$Y^0 = y^{0,N}, \quad Y^1 = y^{1,N},$$

where F is the cost function, and, δ_n is the parameter of the gradient method.

3. We draw a line through two these points, and perform a large step along this line. We have a new point y^{s+1} :

$$y^{s+1} = Y^s + \alpha(Y^s - Y^{s-1}), \quad s = 1, \quad (8)$$

where α is the parameter of the line step.

4. Then we perform some steps from this point by the gradient method, to obtain a new point Y^s :

$$y^{s,n+1} = y^{s,n} - \delta_n \cdot \nabla F(y^{s,n}), \quad (9)$$

$$s = s + 1, \quad Y^s = y^{s,N}.$$

Then step 3 and 4 are repeated with the next values of index s ($s = 2, 3, \dots$).

This optimization algorithm cannot find the global maximum of the cost function, but only a local one. To obtain the better solution of the optimum procedure, it is necessary to analyze N -dimensional volume with different initial points. During the optimization process, it is very important to localize the subspace of the N -dimensional optimization space for more detailed analysis. Then this subspace can be analyzed carefully.

4 Numerical scheme convergence

The numerical scheme for the problem (1) for the DDR IMPATT diode structures was produced some years ago [18]. The scheme analysis showed a very good convergence of the numerical model. The numerical algorithm convergence was obtained during 6–8 high frequency periods. The careful analysis of numerical model for the DAR diode with the doping profile in Fig.1 shows that the numerical

scheme convergence for this type of the doping profile is very slow and the numerical transition process continues many periods to obtain the stationary mode.

The quantitative results of the numerical scheme convergence for the principal diode characteristic, DAR diode conductance as the period number function are shown in Fig. 2.

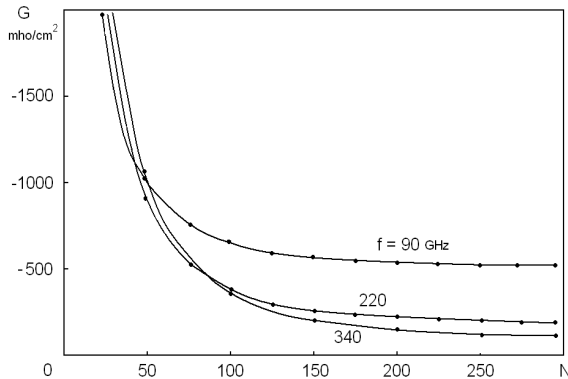


Figure 2. Conductance as function of the period number N .

The necessary number of the consequent periods depends on the diode width and operating frequency and changes from 30 – 50 for the frequency band 15 – 60 GHz up to 150 – 250 periods for 200 – 300 GHz. This very slow convergence was stipulated by the asynchronies movement of the electron and hole avalanches along the same drift region v . It occurs owing to the different drift velocities of the carriers. This effect provokes a large number of necessary periods and large computer time. This is a specific feature of the analyzed type of diode structure.

5 Numerical Results

The accurate analysis for DAR IMPATT diode has been made for different values of p , n and v region width and the different donor and acceptor concentration level. The same doping profile as in [9] gives the negative conductance for very narrow frequency band only, as shown in Fig. 3 in conductance G versus susceptance B plot.

The analysis shows that the active properties of the diode practically are not displayed for more or less significant width of the region v . The solid line of this figure gives dependency for drift layer width $W_v = 0.6 \mu\text{m}$ and the dash line for $W_v = 1.5 \mu\text{m}$. First dependency displays the diode active properties for one narrow frequency band from 50 GHz up to 85 GHz.

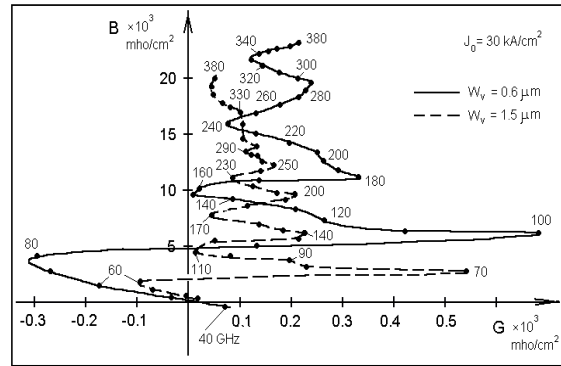


Figure 3. Complex small signal DAR diode admittance for different frequencies and two values of drift layer widths W_v .

Second admittance dependency for $W_v = 1.5 \mu\text{m}$ gives very narrow one frequency band from 40 GHz up to 62 GHz with a vary small value of negative conductance G . In general the admittance behavior has a damp oscillation character but only first peak lies in the negative semi plane. The negative conductance disappears completely for $W_v > 1.5 \mu\text{m}$. The main reason of this effect is a non-synchronize mechanism of carriers' movement along the drift region. This conclusion is contrary to results of the paper [9]. Our results display the active features of the DAR diode the same profile for some frequency bands in case when the v -region width less than $0.5 \mu\text{m}$ only.

One positive idea to increase negative admittance of the diode consists in non-symmetric doping profile utilization. This profile gives some compensation to the asynchronies mechanism. One of the perspective diode structures that was analyzed detail is defined by means of following parameters: the doping level for n and p zone is equal to $0.5_{10}17 \text{ cm}^{-3}$ and $0.2_{10}17 \text{ cm}^{-3}$, accordingly, the widths of the two corresponding areas are equal to $0.1 \mu\text{m}$ and $0.2 \mu\text{m}$, the width of the drift v -region is equal to $0.32 \mu\text{m}$. In Fig. 4 the small signal complex admittance i.e. the conductance versus susceptance is presented for the current density $J_0 = 30 \text{ kA/cm}^2$. It is clear that we can obtain larger value of the conductance increasing the current density.

We can decide that two superior bands appear from the positive conductance G semi plane (look Fig. 3) as a result of the special conditions making for these bands. This effect gives possibility to use superior frequency bands, at least the second band, for the microwave power generation of the sufficient level.

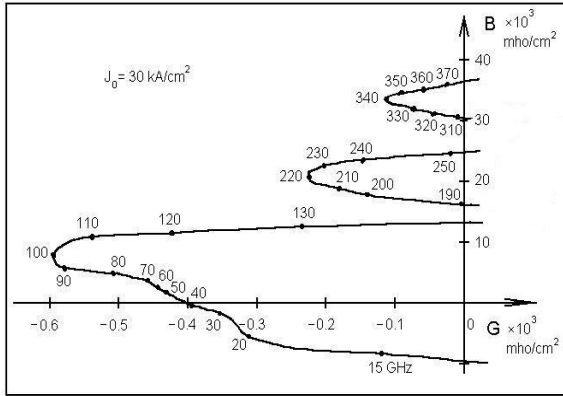


Figure 4. Complex small signal DAR diode admittance for different frequencies and $W_v = 0.32 \mu m$.

The DAR diode internal structure optimization has been provided for the second frequency band near 330 GHz. The cost function of the third frequency band optimization process was selected as output power for the frequency 330 GHz and for two values of the feeding current density as 50 kA/cm² and 70 kA/cm². The results of the analysis and optimization of small signal admittance for third frequency band are shown in Fig. 5 for two current density values: 50 kA/cm² and 70 kA/cm².

The set of the variables for the optimization procedure was composed from five technological parameters of the diode structure: two doping levels for *p* and *n* regions and three widths of *p*, *n* and *v* regions.

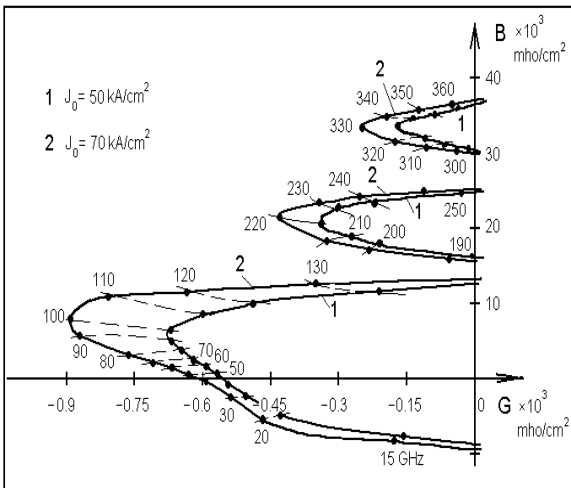


Figure 5. Complex small signal DAR diode admittance optimized for third frequency band for two values of feeding current.

The results of diode structure optimization are presented below for the frequency 330 GHz and feeding current density 50 kA/cm² and 70 kA/cm². The small signal admittance optimization for third frequency band is shown in Fig. 5 for two values of current density: 50 and 70 kA/cm².

The optimal values of these parameters are next: doping levels of *n* and *p* zone are equal to $0.48 \cdot 10^{17} \text{ cm}^{-3}$ and $0.36 \cdot 10^{17} \text{ cm}^{-3}$ accordingly, the widths of the two corresponding areas are equal to $0.09 \mu m$ and $0.18 \mu m$, and the width of the drift *v*-region is equal to $0.32 \mu m$.

The active diode properties for all frequency bands can be improved when the current density increases. More positive effect for this example was obtained for the frequency 330 GHz because of the optimization of the generated power of the diode for this frequency. However it is possible to optimize the conductance and microwave power characteristics for any frequency into the frequency band.

The characteristics obtained for 330 GHz under a large signal serve as the principal result of the analysis. The amplitude characteristics of the conductance for this frequency are shown in Fig. 6 for two values of the current density: 50 kA/cm² and 70 kA/cm².

The active diode properties for all frequency bands are improved when the current density increases. More positive effect was obtained for the frequency 330 GHz because the optimization for this frequency.

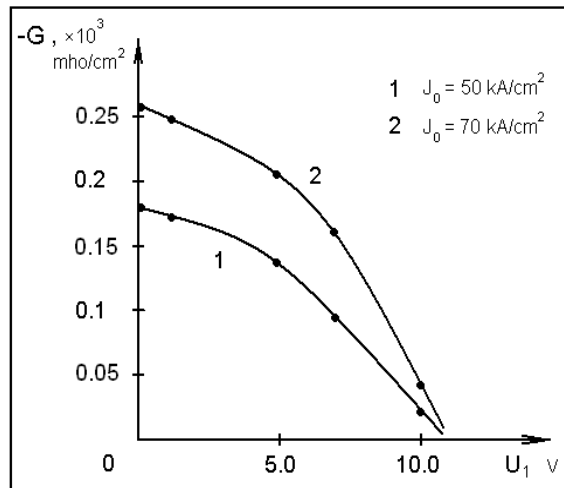


Figure 6. Conductance *G* dependency as functions of first harmonic amplitude U_1 for $f = 330 \text{ GHz}$ and for two values of feeding current density.

The conductance characteristic is softer for current density 50 kA/cm^2 because the diode structure optimization was provided for this current. On the other hand the characteristics for the current density 70 kA/cm^2 are sharper but correspond to the larger conductance $-G$.

The output power dependencies as a function of first harmonic amplitude U_1 for $f = 330 \text{ GHz}$ and for two values of feeding current are shown in Fig. 7.

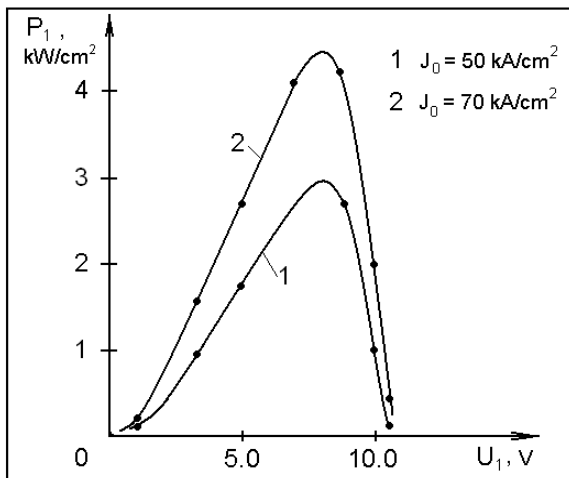


Figure 7. Output generated power P dependency as functions of first harmonic amplitude U_1 for $f = 330 \text{ GHz}$ and for two values of feeding current density.

These amplitude characteristics show the possibility to obtain a sufficient level of output power near the 4 kW/cm^2 for the third frequency band. It means that such a semiconductor structure serves as a perspective source for the microwave power generation in a high frequency band of millimetric region.

6 Conclusion

The numerical scheme that has been developed for the analysis of the different types of IMPATT diodes is suitable for the DAR complex doping profile investigation too. The additional problem that appears for the DAR diode structure analysis is the slower convergence of the numerical model in comparison with the DDR diode analysis.

Some new features of the DAR diode were obtained by the analysis on the basis of nonlinear model. The principal obtained results contradict to the data that were obtained before on the basis of the approximate models of the DAR diode. These results show that the diode does not have the active

properties in some frequency bands for the sufficiently large drift region. To obtain the negative conductance for some frequency bands we need to reduce the drift layer widths to obtain W_v lesser than $0.5 \mu\text{m}$. Nevertheless the diode has a wide first frequency band generation and two superior frequency bands with sufficient output power level. The diode structure optimization gives the possibility to increase the output power level for high frequency bands. This level can be exceeding by the special diode structure optimization taking into account necessary feeding current density.

Acknowledgement

This work was supported by the Puebla Autonomous University, under project VIEP 166/EXC/11-G.

References:

- [1] G. I. Haddad, P. T. Greiling, and W. E. Schroeder, Basic principles and properties of avalanche transit-time devices, *IEEE Trans. Microwave Theory Tech.*, MTT-18, 1970, pp. 752-772.
- [2] K. Chang (Ed.), *Handbook of microwave and optical components*, John Wiley & Sons, New York, 1990.
- [3] M. Tschernitz, and J. Freyer, 140 GHz GaAs Double-Read IMPATT Diodes, *Electron. Lett.*, Vol. 31, No.7, 1995, pp. 582-583.
- [4] W. T. Read, A proposed high-frequency negative resistance diode, *Bell Syst Tech. J.*, Vol. 37, 1958, pp. 401-446.
- [5] B. Som, B. B. Pal, and S. K. Roy, A small signal analysis of an IMPATT device having two avalanche layers interspaced by a drift layer, *Solid-State Electron.*, Vol. 17, 1974, pp. 1029-1038.
- [6] D. N. Datta, B. B. Pal, Generalized small signal analysis of a DAR IMPATT diode", *Solid-State Electron*, Vol. 25, No. 6, 1982, pp. 435-439.
- [7] D. N. Datta, S. P. Pati, J. P. Banerjee, B. B. Pal, and S. K. Roy, Computer analysis of DC field and current-density profiles of DAR IMPATT diode. *IEEE Trans Electron Devices*, Vol. ED-29, No. 11, 1982, pp. 1813-1816.
- [8] S. P. Pati, J. P. Banerjee, and S. K. Roy, High frequency numerical analysis of double avalanche region IMPATT diode, *Semicond Sci Technol*, No. 6, 1991, pp. 777-783.
- [9] A. K. Panda, G. N. Dash, and S. P. Pati, Computer-aided studies on the wide-band microwave characteristics of a silicon double avalanche region diode, *Semicond Sci Technol*, No. 10, 1995, pp. 854-864.

- [10] A. Zemliak, and R. De La Cruz, Comparative analysis of double drift region and double avalanche region IMPATT diodes, *WSEAS Transactions on Commun.*, Vol. 3, No. 1, 2004, pp. 22-27.
- [11] A. Zemliak, and R. De La Cruz, Computer Simulation of a Double Avalanche Region IMPATT Diode, *WSEAS Trans. Circuits Syst.*, Vol. 3, No. 2, 2004, pp. 300-305.
- [12] W. N. Grant, Electron and hole ionization rates in epitaxial silicon at high electric fields, *Solid-State Electron.*, Vol. 16, No. 10, 1973, pp. 1189-1203.
- [13] C. Jacoboni, C. Canali, G. Ottaviani, and A. Alberigi-Quaranta, A review of some charge transport properties of silicon, *Solid-State Electron*, Vol. 20, 1977, pp. 77-89.
- [14] C. Canali, C. Jacoboni, G. Ottaviani, and A. Alberigi-Quaranta, High field diffusion of electrons in silicon, *Appl Phys Lett*, Vol. 27, 1975, p. 278.
- [15] F. Nava, C. Canali, L. Reggiani, D. Gasquet, J.C. Vaissiere, and J.P. Nougier, On diffusivity of holes in silicon, *J Appl Phys*, Vol. 50, 1979, p. 922.
- [16] A.M. Zemliak, Difference scheme stability analysis for IMPATT-diode design, *Izv. VUZ Radioelectronika*, Vol. 24, No. 8, 1981, pp. 831-834.
- [17] A. Zemliak, S. Khotiaintsev, and C. Celaya, Complex nonlinear model for the pulsed-mode IMPATT diode, *Instrumentation and Development*, Vol. 3, No. 8, 1997, pp. 45-52.
- [18] A. Zemliak, C. Celaya, R. Garcia, Active layer parameter optimization for high-power Si 2 mm pulsed IMPATT diode, *Microwave Opt. Technol. Lett.*, Vol. 19, No. 1, 1998, pp. 4-9.